Carbohydrate Polymers 97 (2013) 489–495

Contents lists available at SciVerse ScienceDirect

Carbohydrate Polymers

journal homepage: www.elsevier.com/locate/carbpol

Spray drying: Thermodynamics and Operating Conditions

Valery Normand[a,*], Anandaraman Subramaniam[a], Jeffrey Donnelly[a], Pierre-Etienne Bouquerand[b]

[a] Firmenich Inc., 250 Plainsboro Road, Plainsboro, NJ, USA
[b] Firmenich SA, 7, rue de la Bergère, Meyrin II, GENEVA, CH

ARTICLE INFO

Article history:
Received 12 February 2013
Received in revised form 20 April 2013
Accepted 30 April 2013
Available online 9 May 2013

Keywords:
Maltodextrins
Psychrometric chart
Yield of water evaporation

ABSTRACT

A thermodynamic model has been built to draw a safety envelope of non-stickiness for maltopolymers of various molecular weight distributions. The model is based on the combination of two properties of maltopolymer-water interactions. These interactions include the plasticization and glass formation along with the water sorption properties at different temperatures. The model gives indications on the processing conditions to be used to produce an acceptable powder from a very dilute carbohydrate aqueous solution together with a maximization of the evaporation capacity of the drying equipment.

1. Introduction

Spray drying is a well known and mature technology. While the basic principles of this process may appear to be simple, the process itself can become very complex due to the choice of operating parameters, atmospheric conditions, feed preparation and formulation. Oftentimes appropriate combination of the above factors becomes the responsibility of an experienced expert. However, the process of drying maltopolymer based aqueous solutions can be helped by the use of psychrometric constructions that will guide the process conditions for novices and avoid build up of soft and sticky product in the drying chamber, cyclones and conveying lines.

Stickiness is often a problem in manufacturing operations, especially for mixtures of low molecular weight carbohydrates (e.g. sugars) typical of fruit-juice powders (Brennan, Herrera & Jowitt, 1971; Bhandari, Datta & Howes, 1997; Bhandari, Datta, Crooks, Howes & Rigby, 1997) where it can cause lower production yields. The reason for stickiness is still obscure and mainly linked to the viscosity of the carbohydrate (Downton, Flores-Luna & King, 1982), but stickiness is usually treated empirically (Brennan & Mohamed, 1984).

A reliable estimation of the conditions for which stickiness of carbohydrate materials takes place can be derived from the glass transition temperature (Roos & Karel, 1991a; Roos & Karel, 1991b; Bhandari & Howes, 1999). Even so it is proven that stickiness occurs at a higher temperature for any given water content even for sucrose/fructose mixtures (Adhikari, Howes, Bhandari & Truong, 2001).

For amorphous material the stickiness occurs at the transition between the rubbery state and the liquid state (Downton, Flores-Luna & King, 1982). When considering molecular motion the glass to rubber transition starts when the polymer molecules main back bones become mobile. However due to entanglements, large molecules are not free to migrate from one particle to another until the rubber to liquid transition is reached. In other words stickiness corresponds to the rubber to liquid transition. As the broadness of the rubbery plateau depends of the molecules entanglement (Fox & Flory, 1950; de Gennes, 1979), it becomes very narrow when the polymer has a low polymerisation degree. When low molecular weight materials are considered, the glass to rubber transition temperature is a good approximation for the stickiness temperature. As soon as the temperature reaches the Tg, the molecular mobility rises such that the molecules are not anymore restricted to one particle only.

The purpose of the present work is to develop and utilize a model for stickiness of maltopolymer materials adapted to the drying of low solid concentration solutions. The maltopolymer materials considered in this study are high DE maltodextrins and Glucose syrups that both contain a majority of dimmers and oligomers and a non negligible proportion of large molecular weight species (Normand, Avaltroni and Bouquerand, 2006). Furthermore, the model is used to define the optimal conditions of processing in a conventional dryer. The glass transition temperature is here used as the temperature at which stickiness of the powder might occur, and the model will integrate the modifications of the sorption

* Corresponding author. Corporate R&D Firmenich Inc, 250, Plainsboro Road, Plainsboro, NJ, USA. Tel.: +1 609 580 4457.
E-mail address: valery.normand@firmenich.com (V. Normand).

0144-8617/$ – see front matter © 2013 Elsevier Ltd. All rights reserved.
http://dx.doi.org/10.1016/j.carbpol.2013.04.096

isotherms associated with a temperature change. The article is structured in two parts: I) the model development that is based on maltopolymer-water interactions leading to the construction of the theoretical "*safety envelope*" and II) the determination of the optimal processing conditions that would bring the largest water evaporative capacity taking into consideration the typical atmospheric temperature and humidity conditions at the dryer location. If low molecular weight maltopolymers at low solid concentration in water for the feed solution are considered, the assumption that the kinetics of drying of the droplet does not induce moisture or temperature gradient is acceptable (van Sleeuwen, Zhang, & Normand, 2012).

2. Results and Discussion

2.1. Model development

2.1.1. Building the psychrometric environment:

The psychrometric chart compiles a combination of all elements necessary to guide the operator at defining the optimal process conditions for production. This includes the inlet temperature, the outlet temperature, associated evaporation rate and with more refinements, the water concentration in the feed material.

For clarity reasons only the drying of pure malto-oligomers also called maltodextrins and glucose syrups is considered here.

There are different ways of representing the psychrometric environment. Here we represent the absolute humidity as the horizontal axis and the temperature as the vertical axis. The 100% relative humidity (dew point or appearance of condensation) evolution with temperature is calculated from the Clausius-Clapeyron equation (see Eq.1) where P is the vapour pressure when the temperature is T and P* is the vapour pressure when the temperature is T*, ΔH_{vap} is the enthalpy of vaporisation of water and R is the gas constant.

$$\frac{P}{P^*} = \frac{m}{m^*} = \exp\left(\frac{\Delta H_{vap}}{R}\left(\frac{1}{T} - \frac{1}{T^*}\right)\right) \quad (1)$$

The reference temperatures and pressures are given by the triple point ($P^* = 6.10^{-3}$ atm; $T^* = 273.16$ K; $\Delta H_{vap} = 45.05$ kJ.mol^{-1}) for temperatures lower than 50 °C and by the boiling point for temperature higher ($P^* = 1.00$ atm; $T^* = 373.15$ K; $\Delta H_{vap} = 40.66$ kJ.mol^{-1}). It is also assumed here that the enthalpy of vaporisation from 273.16 K to 373.15 K decreases linearly with the temperature, which becomes a fair approximation considering the amplitude of the enthalpy change within this temperature range.

Then, for a given temperature, the relative humidity value is simply the percentage of the 100% pressure as calculated using Eq.1. This generates a family of curves of increasing temperature when absolute humidity increases. For temperatures below the dew point, water condensation occurs.

During evaporation of water, the temperature drops due to the adiabatic state change of water (Kloppers & Kröger, 2005). The temperature drop (ΔT) follows Eq.2 where m_{air} and m_w are the mass of dry air and water respectively, Q is the sensible heat and ΔH_{vap} is the latent heat (-2258.7 kJ/kg).

$$\Delta T = m_{air} Q + m_w \Delta H_{vap} \quad (2)$$

2.1.2. Building the "safety envelope":

What here is called the "*safety envelope*" is a surface in a psychrometric environment in which stickiness of the powder cannot occur. The envelope is delimited by the line that separates two states of motion, one of slow mobility and the other of fast mobility. It is here simplified to the Tg/water activity relationship but could easily be adapted to more complex definition of the stickiness as authors mentioned that stickiness might occur between 0 and 10 to 20 °C above the Tg (Downton *et al.*, 1982; Adhikari, Howes, Bhandari & Truong, 2001). Those data are not easily measurable and a combination of two properties is here preferred that is the Tg/water content relationship and the water activity/water content relationship for a given material as first attempted by Roos (Roos, 1993). Fortunately, such data is readily available in the literature for commonly used spray drying raw materials and are reported in Table 1 for a set of maltodextrins and glucose syrup samples.

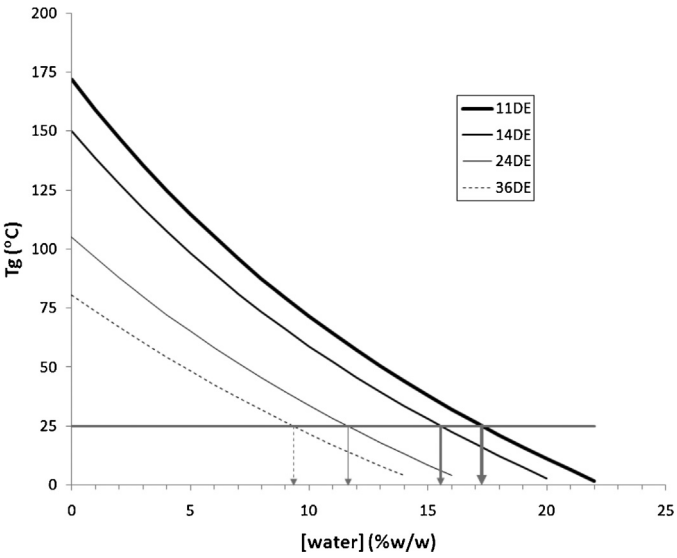

Figure 1. Glass transition of maltopolymers of various DE as a function of the water content. The arrows materialize the water content of the maltodextrin that separates the glass to rubber states at 25 °C.

2.1.2.1. Tg/water content. The Tg/water content relationship of maltodextrins has been reported a number of times (Orford, Parker, Ring, & Smith, 1989; Roos & Karel, 1991a; Roos & Karel, 1991b; D'Haene & Van Liederkerke, 1996) based on original contributions (Couchman, 1978; Couchman & Karasz, 1978). Furthermore, a predictive model has been suggested to link the distribution of molecular weight to the Tg in the absence of water (Avaltroni, Bouquerand, & Normand, 2004; Normand et al., 2006).

The relationship is described in Eq.3 when ω is the water weight fraction of the sample, Tg is the glass transition and ΔCp is the calorific capacity increment for the transition:

$$T_{g\,mixture} = \frac{\omega \Delta C_{pW} T_{gW} + (1-\omega)\,\Delta C_{pmalto} T_{g\,dry}}{\omega \Delta C_{pW} + (1-\omega)\,\Delta C_{pmalto}} \quad (3)$$

Usually, the representation of Tg/water content is a phase diagram that separates a glass from a rubber like material as shown in Fig. 1 for a series of maltopolymers of various Dextrose Equivalent (DE).

2.1.2.2. Water content/water activity:. The water content/water activity relationship is typical of sorption isotherms. Those have been well described by Radosta, Schierbaum, Reuther, & Anger (1989), using Guggenheim Anderson de Boer (GAB) formalism (Anderson, 1946; Guggenheim, 1966; De Boer, 1968), for maltodextrins of controlled molecular weight leading to a thermodynamic understanding of the sorption (Normand & Bouquerand, 2007).

Table 1
Description of the maltopolymers used as examples and the relevant properties associated to the glass transition temperature and sorption isotherms. The determination of the GAB parameters (K, C and X_m) used for the construction of the isotherms at various temperatures is made using the Arrhenius equations published in Normand & Bouquerand, 2007.

	11DE	14DE	24DE	36DE	reference
Carbohydrate Characterization					
DE real	10.9	13.8	23.8	36.2	Subramaniam, 1984
Mn	1505	1194	698	466	Subramaniam, 1984
Couchman's parameters					
T_g dry	172	150	105	80.7	Subramaniam, 1984
ΔCp	0.447	0.463	0.517	0.582	Avaltroni *et al.*, 2004
GAB's parameters					
Xm_0	0.0615	0.0573	0.0486	0.0429	Radosta *et al.*, 1989
K_0	0.1364	0.1265	0.0952	0.0647	Radosta *et al.*, 1989
C_0	25.596	28.553	38.87	51.53	Radosta *et al.*, 1989
ΔH_{lp}	552.1	591.7	729.9	899.6	Radosta *et al.*, 1989
ΔH_{mp}	28.53	25.81	19.47	14.64	Radosta *et al.*, 1989

The sorption isotherm is well described by the GAB empirical model, where X_W is the water content on a dry basis and X_m, K and C are empirical constants whereas a_W is the water activity (see Eq.4):

$$X_W = \frac{X_m K C a_W}{(1 - K a_W)(1 - K a_W + K C a_W)} \quad (4)$$

A representation of the water isotherms of sorption is shown in Fig. 2. Combining Eqs.3 and 4, an estimation of the water activity for which the Tg will be the temperature of the isotherm becomes achievable. The water activity at this point is also called the critical water activity (a_w*) and corresponds to a critical relative humidity (RH*) at the same temperature (Bouquerand, Maio, Meyer, & Normand, 2008; Sillick & Gregson, 2010). The RH* is highlighted in Fig. 2 by the vertical arrows.

In Fig. 2, the higher the DE and the lower the capacity to stabilize water under low relative humidity conditions, whereas the sorption isotherm increases abruptly under elevated relative humidity conditions. Also, the lower the DE, the more capacity to store water under low RH conditions.

A simplified relationship is obtained when combining Couchman (Eq.3) and GAB (Eq.4) models that represent the glass transition temperature as a function of the relative humidity.

The analytical combination of Eq.3 and Eq.4 leads to the expression of a_w as a function of the GAB parameters (see Eq.5).

$$a_W = \frac{X_W K (2 - C) + X_m K C - \sqrt{[X_W K (C - 2) - X_m K C]^2 - 4 X_W^2 K^2 (1 - C)}}{2 X_W K^2 (1 - C)} \quad (5)$$

Where X_W is calculated using Eq.6.

$$X_W = \frac{[W]}{1 - [W]} = \frac{\Delta C_{pmalto} \left(Tg_{dry} - Tg\right)}{\Delta C_{pW} \left(Tg - Tg_W\right)} \quad (6)$$

Furthermore the arrows in Fig. 3 are the result of Eq.7 for X_W, Xm, K and C being the GAB parameters values at 25 °C.

$$a_W^* = \frac{X_W K (2 - C) + X_m K C - \sqrt{[X_W K (C - 2) - X_m K C]^2 - 4 X_W^2 K^2 (1 - C)}}{2 X_W K^2 (1 - C)} \quad (7)$$

Equation 5 allows the construction of a Tg: a_w representation (see Fig. 3).

The recorded a_w* as calculated for this specific set of maltopolymers (with various distributions of molecular weights) are then compared to reported measured values and extrapolation of those in Fig. 4. The range of Dextrose Equivalent (DE) expressed in the literature is comparable to the range of DE used in calculation.

According to the data shown in Fig. 4, the theoretical model that links the RH* to the DE of the maltodextrin is consistent. However, it is obvious that the sorption isotherm changes when the

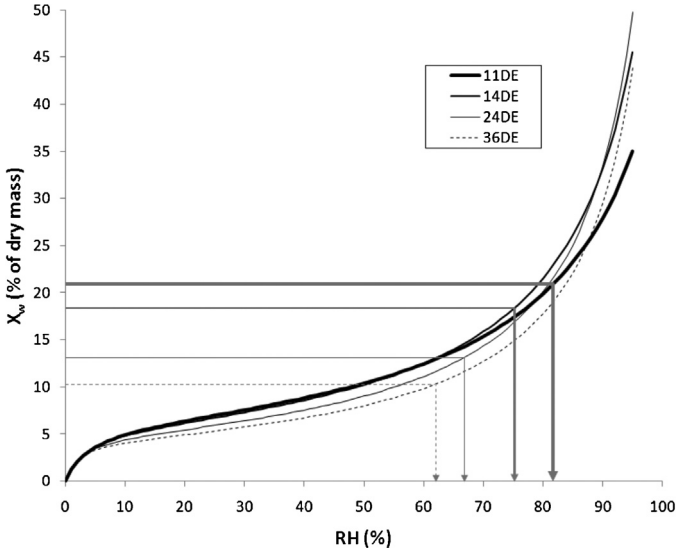

Figure 2. Isotherms of sorption for the identical series of maltopolymers presented in Fig. 1. Isotherms have been calculated using the relationships described in Normand & Bouquerand, 2007 from data reported in Radosta et al., 1989. The red arrows materialize the critical relative humidity at 25 °C by reporting the water content necessary to reach the Tg at 25 °C (see Fig. 1).

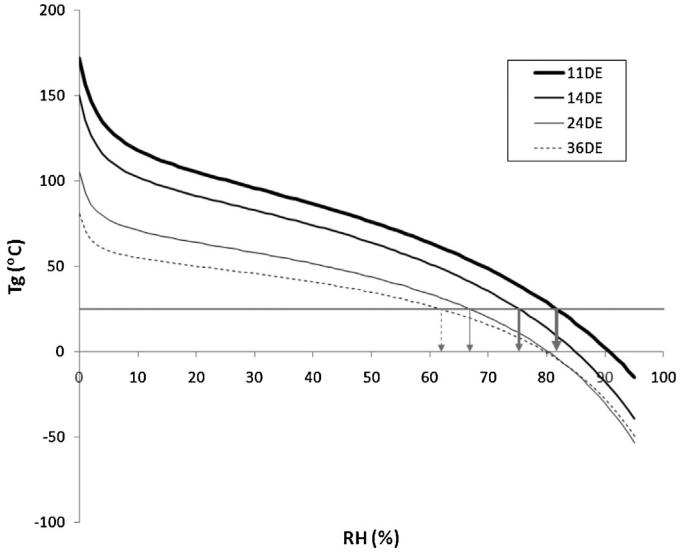

Figure 3. Isotherms of sorption for the identical series of maltopolymers presented in Fig. 1 and 2 representing the Tg as a function of the relative humidity. The arrows materialize the critical relative humidity at 25 °C by reporting the RH* necessary to reach the Tg at 25 °C (see Figs. 1 and 2).

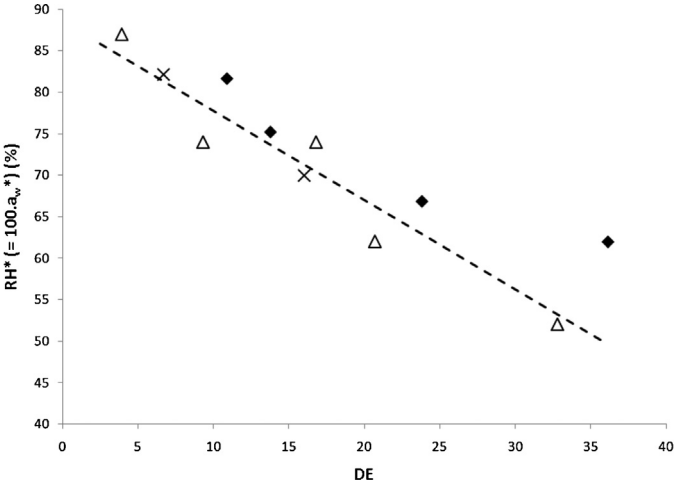

Figure 4. Comparison between a_w* calculated (plain diamonds, this work) and a_w* reported measured values in the literature as a function of the dextrose equivalent; triangles (Subramaniam, 1984) and crosses and dashed line (Sillick & Gregson, 2010).

temperature changes which has been demonstrated and reported several times (Radosta et al., 1989). Only the three parameters (Xm, K and C) of the GAB equation (Eq.4) are affected by the molecular weight distribution and the temperature. The relevant Arrhenius relationships have been expressed, discussed and successfully used elsewhere (Normand & Bouquerand, 2007). To achieve the contour of the "*safety envelope*", one needs to have as many isotherms as temperatures required for the required quality of the curve. However, only one data point per isotherm is useful, that is when the water activity separates the two states (glassy/rubbery).

The Arrhenius relationships allow estimation of the sorption isotherms at various temperatures, and Eq.7 is still valid to determine the critical relative humidity.

An example is given in Fig. 5 for an 11DE maltopolymer sorption isotherms series at 5 different temperatures in Fig. 7 using the Arrhenius parameters extrapolated from Radosta et al. (1989).

In Fig. 5, the hotter the temperature, the less steep is the isotherm under high relative humidity conditions. However, under low relative humidity conditions, the isotherm is not very much affected by the temperature. Meanwhile, the glass to rubber transition occurs at elevated water concentrations, and therefore in the most temperature sensitive part of the sorption isotherm.

2.1.2.3. Constructing the "safety envelope" for maltopolymers:. It has been shown previously that all three GAB parameters evolve with the temperature and can be expressed as an Arrhenius relationship (Normand & Bouquerand, 2007 from data reported in Radosta et al., 1989). In the present construction, the same numerical values are used. Therefore, for each Tg corresponding to each isotherm measurement temperature, one and only one a_w* (Bouquerand et al., 2008; Sillick & Gregson, 2010) is determined.

Now, for each combination of a_w* and temperature corresponds one absolute humidity value calculated using Eq.1 and replacing P/P* by a_w*.

This generates the continuous fit in Fig. 6 for all maltopolymer carrier systems introduced earlier in this article. The safe area is inside the curve (on the left hand side), the material is a solid glass and outside the boundary (on the right hand side), the material is rubbery due to enhanced molecular mobility.

The characteristics of the safety envelope (area under the curve, apex temperature for largest absolute humidity, maximum absolute humidity. . .) fit perfectly with the number average molecular weight of the maltopolymer as shown in Fig. 7a,b,c.

In Fig. 7, it is shown that the shape of the safety envelop is homothetic and depends exclusively on the number average molecular weight of the maltopolymer.

2.1.2.4. Thermodynamical determination of operating drying conditions:. The 3 important operating conditions:

There are three strategic "temperature/absolute humidity" conditions represented on a psychrometric chart that are related to successful process conditions. Those are the starting air properties (Temperature and RH), that is the air that is taken to dry the substance, the heated air temperature (inlet conditions) and the final air conditions (outlet conditions). The outlet conditions (air temperature and air humidity) influence the product aspect and also the inlet air temperature whereas the initial air relative humidity dictates the inlet air humidity content.

2.1.2.4.1. The initial air properties:. The initial air conditions are either controlled (presence of a dehumidifier) or not (air taken straight from outside a plant and filtered for impurities to avoid contamination). High inlet air humidity can be detrimental to the drying capacity of the dryer. When the molecular weight of the product to dry is small such conditions can lead to sticking of the powder in the dryer. In Fig. 8, the air properties during spring or fall seasons are given for Newark airport, NJ. The dryers in the example are not equipped with a dehumidifier. The air taken (circle in Fig. 8)

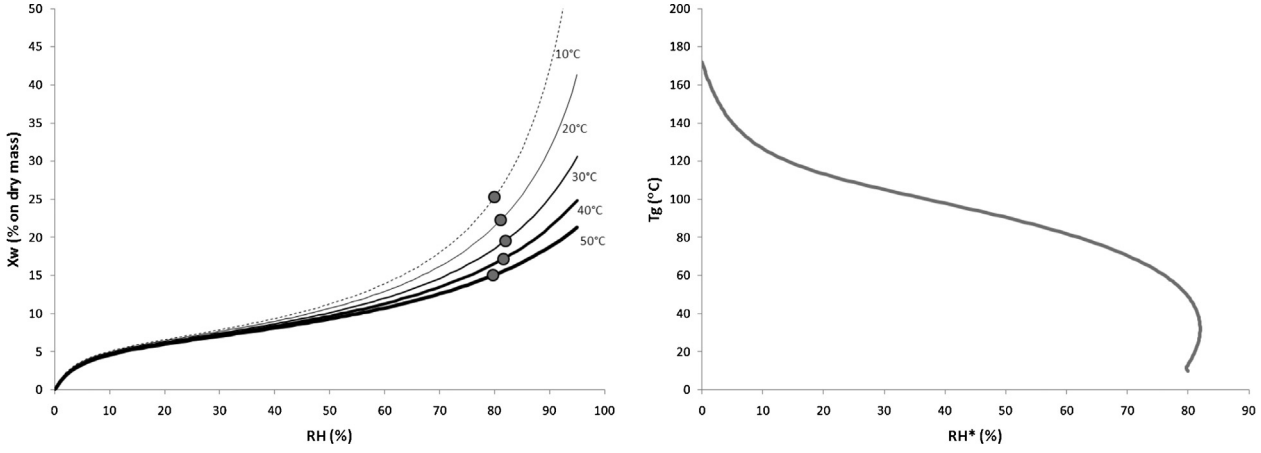

Figure 5. Left shows isotherms of sorption at different temperatures ranging from 10 to 50 °C using the Arrhenius relationships published in Radosta et al., 1989 (series of black curves) for an 11DE maltopolymer sample and localization of the glass to rubber transition occurring at RH = RH* and materialized by grey circles. Right shows the continuous Tg–RH* relationship for the same material.

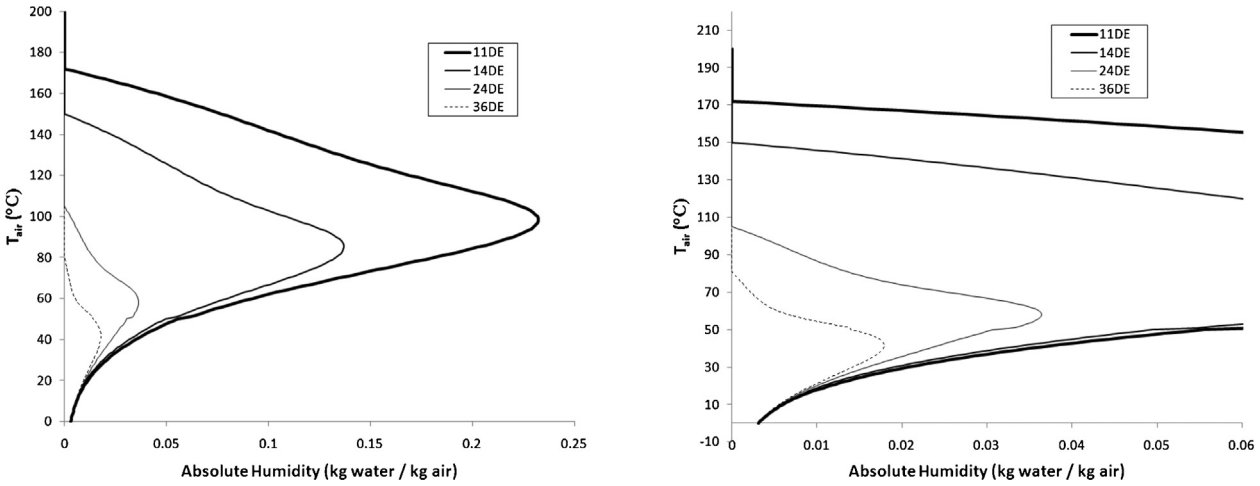

Figure 6. Left: Curves separating the glassy state from the rubbery state for different DE maltopolymers under different temperature and humidity conditions for the headspace. Inside the envelope the material is glassy. Outside the envelope the material is rubbery. Right: Representation of the figure on the left at larger scale.

is at 25 °C and 50% relative humidity corresponding to a dew point of 13.5 °C.

2.1.2.4.2. Determination of the outlet Temperature and absolute humidity conditions:. The outlet temperature has to be determined so that the dry particles generated are non-sticky to avoid coating of the dryer wall resulting in a long residence time leading to caking. Therefore the outlet temperature and absolute humidity conditions have to be chosen inside the "*safety envelope*". The absolute humidity of the outlet air is driven by the quantity of water that is evaporated in the dryer. Though, a direct relationship between the water content of the carbohydrate solution (dryer feed) and the feed rate are not critical to over drying nor under drying, both can

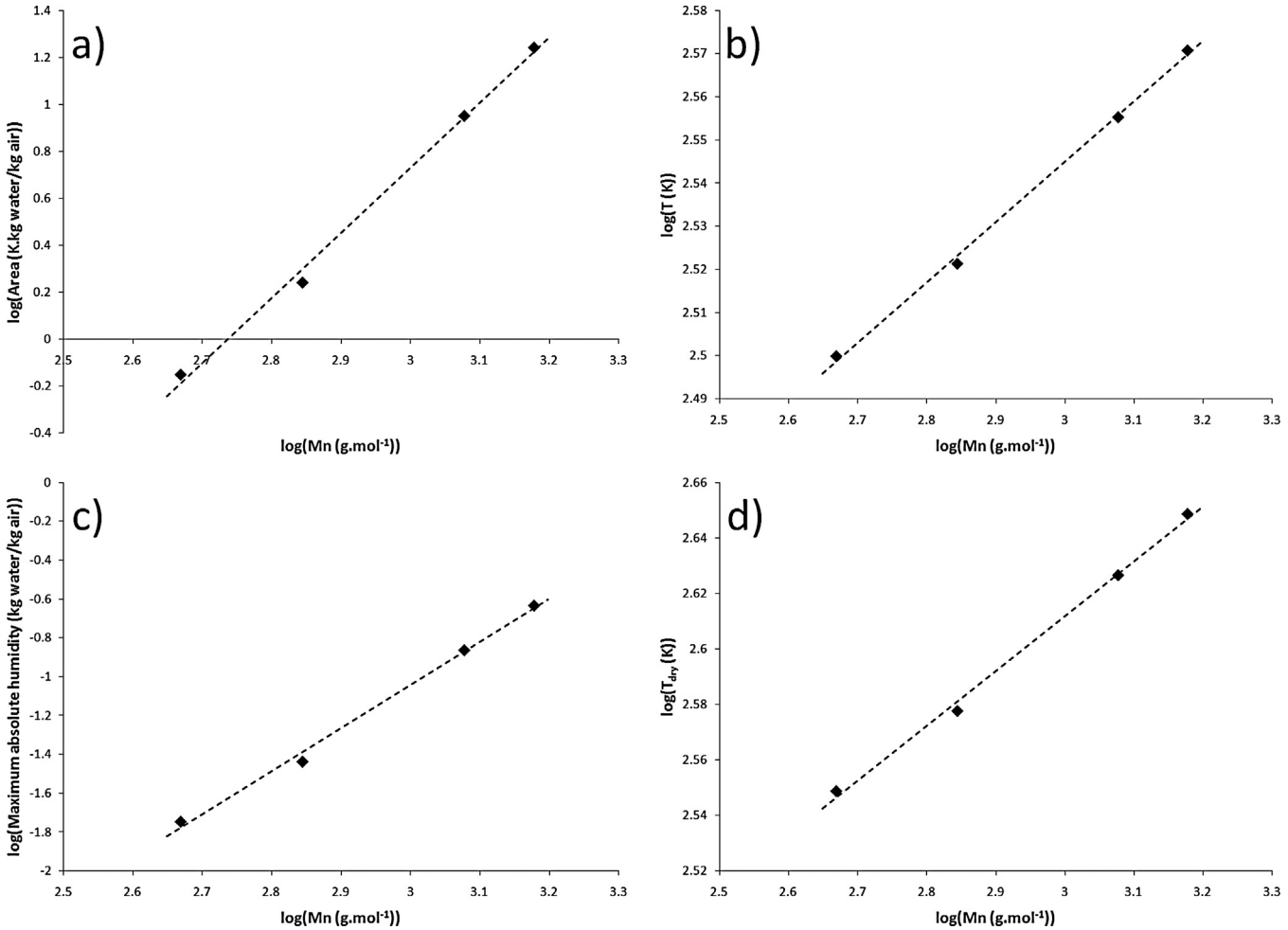

Figure 7. a) Area, b) absolute temperature at the apex c) amplitude of the apex of the curves represented in Fig. 6 and d) absolute Tg_{dry} as a function of the number average molecular weight of the maltopolymer. Dashed lines are for guiding the eyes.

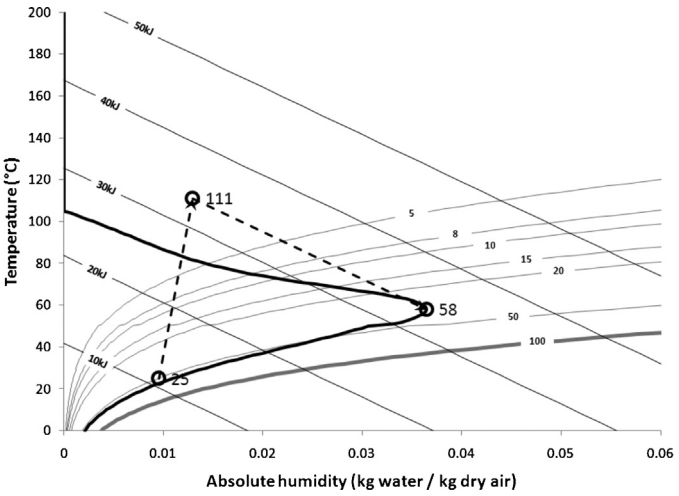

Figure 8. Inlet conditions determined by atmospheric outside conditions (circle at 25 °C and 50% relative humidity) and optimal outlet air conditions determined by the "safety envelope" (circle at 58 °C and 33.2% relative humidity) to optimize the throughput of a non-sticky 24DE based powder. The upward dashed line represents the increase in absolute humidity of the air when heated by direct burner gas. The downward dashed line represents the adiabatic cooling path to end up with the optimal outlet conditions. The two dashed lines cross at 111 °C which is the optimized inlet temperature. The 100 line is the dew point temperature and the grey lines correspond to the relative humidity.

contribute to outlet conditions lying outside the "*safety envelope*". In Fig. 8, the outlet temperature and absolute humidity should be as far as possible from the y-axis so that the outlet air carries the maximum humidity. The outlet temperature and absolute humidity should be inside the "*safety envelope*" for producing a non-sticky powder. The located best conditions for the outlet temperature (circle at 58 °C and 33.2% relative humidity) belong to an adiabatic cooling curve represented by the downward dashed line in Fig. 8.

2.1.2.4.3. The inlet air conditions:. The inlet air drawn from outside the plant (see point 1) and is heated by a direct methane fired furnace. The combustion products are primarily water and carbon dioxide. The water generated for heating 1 kg of air corresponds to 0.04 g/K. This quantity will be added to the water already contained in the initial air. This humidification of the air upon heating is represented as the upward dashed line in Fig. 8.

The targeted inlet air temperature should be the intersection of the two dashed lines (the upward and the downward) in Fig. 8.

The maximum water evaporation capacity is read on Fig. 8 as the difference between the outlet absolute humidity conditions and the inlet absolute humidity conditions multiplied by the inlet air flow rate that is 6900 kg of air/hr for a 250 kg of water/hr evaporation rate capacity medium size dryer. It corresponds to 162 kg of water/hr evaporated. It should be stressed here that the feed rate condition has to be appropriately adjusted.

Now if summer weather is considered in the same area, the average temperature is 35 °C and the relative humidity is 70% corresponding to a dew point of 28.5 °C, the evaporation capacity drops to 78 kg of water/hr evaporation rate. Also, the inlet air temperature is now 84 °C compared to the 111 °C observed in spring or falls for the same outlet temperature of 58 °C.

When a 14DE maltodextrin aqueous solution is considered to be dried, the "*safety envelope*" is wider than for the 24DE shown in Fig. 8 and full capacity of the dryer is obtained without problem. However, the modification of the operating conditions will certainly affect other properties than the stickiness of the final powder: density, size, shape to name a few.

3. Conclusion

A psychrometric model has been developed based on the thermodynamics of polymer–water interactions. The glass transition temperature separating glassy to rubbery states, was used as a measure to determine the "*safety envelope*" for a series of maltopolymers. The model is based on the combination of the Couchman equation, the GAB sorption isotherm equation and the temperature dependence of the GAB sorption isotherm. The model is proposed to estimate the two optimal operating temperatures to be used in a conventional dryer.

However, the process of drying carbohydrate aqueous solution is not only related to the thermodynamics but is also kinetics dependent. The thermodynamic model itself does not account for the kinetics of water redistribution within a liquid droplet of the feed emulsion. The kinetics associated with the thermodynamics will result in a wider "*safety envelope*" which puts the present model on the safe side of the physics of drying. Further work on the topic is necessary to ultimately predict the drying conditions of very low molecular weight carbohydrate solutions. To do so, a careful study describing the stickiness temperature variation with the molecular weight distribution of the carbohydrate to be dried is needed and a predictive model for stickiness should be constructed.

References

Adhikari, B., Howes, T., Bhandari, B. R., & Truong, V. (2001). Stickiness in foods: a review of mechanisms and test methods. *International Journal of Food Properties*, *4*(1), 1–33.

Anderson, R. B. (1946). Modifications of the Brunauer, Emmett and Teller Equation. *J. Am. Chem. Soc.*, *68*, 686–691.

Avaltroni, F., Bouquerand, P.-E., & Normand, V. (2004). Maltodextrin molecular weight distribution influence on the glass transition temperature and viscosity in aqueous solutions. *Carbohydrate Polymers*, *58*(3), 323–334.

Bhandari, B. R., Datta, N., & Howes, T. (1997). Problems associated with spray drying of sugar rich foods. *Drying Technologies*, *15*(2), 671–684.

Bhandari, B. R., Datta, N., Crooks, R., Howes, T., & Rigby, S. (1997). A semi empirical approach to optimize the quantity of drying aids required to spray dry sugar rich foods. *Drying Technologies*, *15*(10), 2509–2525.

Bhandari, B. R., & Howes, T. (1999). Implication of glass transition for the drying and stability of foods. *J. Food Eng.*, *40*(1–2), 71–79.

Bouquerand, P.-E., Maio, S., Meyer, F., & Normand, V. (2008). Moisture stability of maltodextrin based delivery systems. *Food Biophysics*, *3*(3), 182–185.

Brennan, J. G., Herrera, J., & Jowitt, R. (1971). A study of some of the factors affecting the spray drying of concentrated orange juice, on a laboratory scale. *Food Technologies*, *6*, 295–307.

Brennan, J. G., & Mohamed, A. M. A. (1984). Relating sensory stickiness and physical properties of foods. In B. M. MacKenna (Ed.), *In Engineering and Food* (1) (pp. 489–498).

Couchman, P. R. (1978). Compositional variation of glass-transition temperature. 2. Application of the thermodynamic theory to compatible polymer blends. *Macromolecules*, *11*(6), 1156–1161.

Couchman, P. R., & Karasz, F. E. (1978). A classical thermodynamic discussion of the effect of composition on glass-transition temperature. *Macromolecules*, *11*(1), 117–119.

De Boer, J. H. (1968). *The Dynamical Character of Adsorption* (2nd Ed, pp.). Oxford: Clarendon Press.

de Gennes, P. G. (1979). *Scaling Concepts in Polymer Physics*. Cornell: University Press.

D'Haene, P., & Van Liederkerke, B. (1996). Viscosity prediction of starch hydrolysates from single point measurements. *Starch/Stärke*, *48*(9), 327–334.

Downton, G. E., Flores-Luna, J. L., & King, C. J. (1982). Mechanism of stickiness in hygroscopic, amorphous powders. *Ind. Eng. Chem. Fundam.*, *21*, 447–451.

Fox, T. G., & Flory, P. J. (1950). Second-order transition temperatures and related properties of polystyrene. 1. Influence of molecular weight. *J. Applied Phys.*, *21*, 581–591.

Guggenheim, E. A. (1966). *Applications of Statistical Mechanics*. Oxford: Clarendon Press.

Kloppers, J. C., & Kröger, D. G. (2005). A critical investigation into the heat and mass transfer analysis of counterflow wet-cooling towers. *Int. J. Heat and Mass Transfer*, *48*, 765–777.

Normand, V., Avaltroni, F., & Bouquerand, P.-E. (2006). Mathematical discretisation of Size-Exclusion-Chromatograms applied to commercial corn maltodextrins. *Journal of Chromatographic Science*, *44*(2), 91–95.

Normand, V., & Bouquerand, P.-E. (2007). Dimensionless hygroscopic number of malto-oligomers. *Starch/Stärke*, *59*(2), 100–102.

Orford, P. D., Parker, R., Ring, S. G., & Smith, A. C. (1989). Effect of water as a diluent on the glass transition behaviour of malto oligosaccharides, amylose and amylopectin. *International Journal of Biological Macromolecules*, *11*, 91–96.

Radosta, S., Schierbaum, F., Reuther, F., & Anger, H. (1989). Polymer-Water Interaction of Maltodextrins, Part I: Water Vapour Sorption and Desorption of Maltodextrin Powders. *Starch/Stärke*, *41*, 395–401.

Roos, Y., & Karel, M. (1991a). Phase transitions of mixtures of amorphous polysaccharides and sugars. *Biotechnol. Prog.*, *7*, 49–53.

Roos, Y., & Karel, M. (1991b). Water and molecular weight effects on glass transitions in amorphous carbohydrates and carbohydrate solutions. *J. Food Sci.*, *56*(6), 1676–1681.

Roos, Y. H. (1993). Water activity and physical state effects on amorphous food stability. *J. Food Processing and Preservation*, *16*, 433–447.

Sillick, M., & Gregson, C. M. (2010). Critical water activity of disaccharides/maltodextrin blends. *Carbohydrate Polymers*, *79*, 1028–1033.

van Sleeuwen, R. M. T., Zhang, S., & Normand, V. (2012). Spatial Glass Transition Temperature Variations in Polymer Glass: Application to a Maltodextrin-Water System. *Biomacromolecules*, *13*(3), 787–797.